รหัสโครงการ SUT 1-103-43-12-05

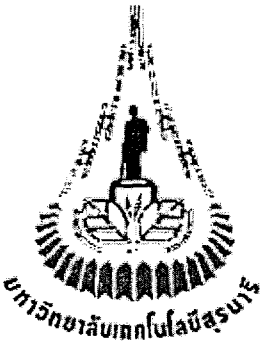

รายงานการวิจัย

The Numerical Simulation of the Incompressible Viscous Fluid Flow with Prescribed Pressure Drop Through Helical Tube

การจำลองระเบียบวิธีเชิงตัวเลขสำหรับการไหลของของไหลที่มีความหนืดและไม่อัดตัวโดยให้ค่าความดันที่ลดลงผ่านท่อเกลียว

ผู้วิจัย

Associate Professor Dr. Nikolay Pavlovich Moshkin
School of Mathematics
Institute of Science
Suranaree University of Technology

ได้รับทุนอุดหนุนการวิจัยจากมหาวิทยาลัยเทคโนโลยีสุรนารี ปีงบประมาณ พ.ศ.2543
พฤษภาคม 2546

รหัสโครงการ SUT 1-103-43-12-05

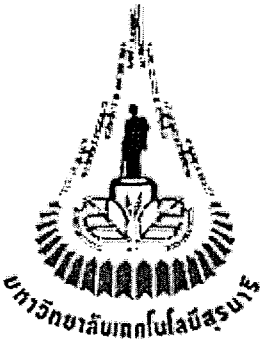

รายงานการวิจัย

The Numerical Simulation of the Incompressible Viscous Fluid Flow with Prescribed Pressure Drop Through Helical Tube

การจำลองระเบียบวิธีเชิงตัวเลขสำหรับการไหลของของไหลที่มีความหนืดและไม่อัดตัวโดยให้ค่าความดันที่ลดลงผ่านท่อเกลียว

ผู้วิจัย

Associate Professor Dr. Nikolay Pavlovich Moshkin
School of Mathematics
Institute of Science
Suranaree University of Technology

ได้รับทุนอุดหนุนการวิจัยจากมหาวิทยาลัยเทคโนโลยีสุรนารี ปีงบประมาณ พ.ศ.2543
พฤษภาคม 2546

ACKNOWLEDGEMENT

This is to acknowledge to the Suranaree University of Technology Research Fund Administration for financial support of this project.

ABSTRACT

This project was a first, preliminary part of the project to study viscous incompressible fluid flow in helical circular pipes under given pressure drop. In this report a set of incompressible viscous fluid mechanics equations in an arbitrary curvilinear coordinate system are presented. The form of the Navier-Stokes equations in helical coordinate system was obtained as particular case.

บทคัดย่อ

โครงงานวิจัยนี้เป็นส่วนหนึ่งของการศึกษาการไหลของของไหลที่มีความหนืด และไม่อัดตัวโดยให้ค่าความดันที่ลดลงผ่านท่อเกลียว ในรายงานการวิจัยนี้ได้นำแสนอระบบสมการกลศาสตร์ของของไหล(ระบบสมการนาเวียร์-สโตก) ที่มีความหนืดและอัดตัวไม่ได้ บนระบบพิกัดเชิงเส้นโค้ง เราสามารถจัดระบบสมการนาเวียร์-สโตกนี้บนระบบพิกัดของเฮลิเคิล

CONTENTS

1. Introduction

1.1 Background

Helical pipes are used extensively in various industrial applications, especially in cooling or heating devices. In the research of biological fluid mechanics, blood vessels are also typically curved pipes. It is verified experimentally in Ref. [1] that secondary flow affects the various aspects of the fluid flow in curved pipes considerably. For its importance, many efforts have been made in this field. However, because of its complexity, there exist many problems to be solved as indicated Refs. [2,3].

The previous researches on this subject can be briefly divided into three stages. The first stage was emphasized on the finding of the secondary flow. In the second stage, the early analytical work was done by Dean Ref. [4], who studied the flow in planar curved pipe using a concentric toroidal coordinate system. Afterwards, numerous authors utilized Dean's coordinates to investigate the flow in toroidal pipes. Subsequently, in third stage, the study of flow in curved pipes with non-zero torsion as helical pipes deserves attention. However, so far most research efforts focused on planar curved pipe flows, studies on the flow in helical pipes are relatively limited.

In those previous studies of helical pipe flows, Murata et al. [5], Wang [6] and Germano [7] did the fundamental investigation. Although some differences exist in their results such as the order of the torsion effect, they have successfully deduced the Navier-Stokes equations in a non-orthogonal or orthogonal coordinate system, respectively. Now their works are being carried further and some attitudes have been put forward to solving the disagreements between them. For instance, like Masliyah [8] and Murata et al. [5] and Kao [9] found that the definition of stream function cannot reflect the strength of the secondary flow, which must be illustrated by corresponding velocity vectors. Comparing the results derived with series expression and numerical methods, Kao tried to address the paradox between Wang and Murata et al. and Germano. However, the mechanism of the torsion effect is still not clear. After detailed interpretation of the relationship between the two coordinate systems used by Wang and Germano, in Ref. [10] Tuttle solved the flow in pipes of elliptical cross-section and circular cross-section, successively. Then he qualitatively stated that the order of the torsion effect on secondary flow depended on the frame of reference of the observer. Without any approximation in the governing equations, Chen [11] obtained the flow solutions for helical circular pipes by the double series expansion method. But considering the series forms of dimensionless axial velocity and stream function used in his article, the method also has the same drawbacks as perturbation technique.

In the literature, the commonly used methods are theoretical analysis and numerical discretization. It is known that the analytical techniques have the major advantage over numerical discretization techniques of providing physical insight into the nature of the solution of the problem. Perturbation technique, as an approximately theoretical analytical technique, is the most important method used in this field. Despite its usefulness, perturbation technique also has two major drawbacks. Firstly, for practical applications, the perturbation series has to be restricted to few terms; secondly, in order to obtain solutions of acceptable accuracy, the perturbation parameters are limited to be small. And as one of the methods of weighted residuals, Galerkin technique might overcome these limitations and obtain high-order semianlytical solutions that are unavailable by direct numerical discretization as pointed Ref. [12].

To sharpen the focus of the study and to avoid the complication connected with the interpretation of covariant and contra-variant velocity components, Germano's orthogonal coordinate system is employed in the present work.

1.2 Objectives

The objectives of the project were:
1) To formulate the mathematical model of fluid flow through coiled pipes with prescribed pressure drop.
2) To find analytical or approximate solution of the above problem for fully developed flow in helical pipe.

1.3 Hypothesis

The main hypothesis in such kind of an investigation is that fluid is viscous incompressible, the mass forces are equal to zero and the governing equations are the Navier-Stokes equations.

1.4 Usefulness and benefits

The immediate beneficiaries of this project are the mathematical model (Navier-Stokes equations in curvilinear and helical coordinate systems) which may be useful for modeling internal fluid flows in curved pipes.
Longer term results of this project are the following:

- It can be used by researchers doing numerical modeling of internal fluid flow through curve pipes;
- It can be used to find the dependence between pressure drop and mass flow rate of flow through curve pipe.

1.5 Scope and limitations.

The present research describe the mathematical models of fluid flow within curve duct on the example of viscous incompressible flow in helical pipe. We will consider only the flow for which on the inflow and outflow section of duct the value of pressure and tangent component of velocity are known us boundary conditions.

2. Navier-Stokes equation in orthogonal coordinate system.

Consider an arbitrary space curve described by (see Figure 1)

$$R(s) = F_x(s)\mathbf{i} + F_y(s)\mathbf{j} + F_z(s)\mathbf{k} \tag{1}$$

where $\mathbf{i},\mathbf{j},\mathbf{k}$ are unite vectors and s is the arclength along the curve, $F_x(s)$, $F_y(s)$, $F_x(s)$ are functions of s. The Frenet triad of unit vectors $\mathbf{T},\mathbf{N},\mathbf{B}$ can be given

$$\mathbf{T} = \frac{d\mathbf{R}}{ds},\ \mathbf{N} = \frac{1}{k}\frac{d\mathbf{T}}{ds},\ \mathbf{B} = \mathbf{T}\times\mathbf{N} \tag{2}$$

and the Frenet formulas are used

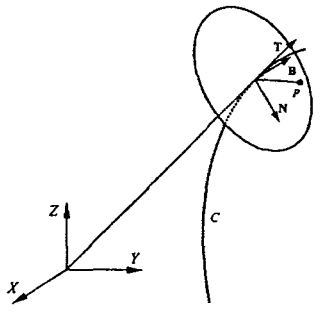

Fig. 1. Sckech of Frenet triad for an arbitrary curve in space.

$$\frac{d\mathbf{N}}{ds} = -k\mathbf{T} + \tau\mathbf{B}, \quad \frac{d\mathbf{B}}{ds} = -\tau\mathbf{N}, \quad \frac{d\mathbf{T}}{ds} = -k\mathbf{N}. \tag{3}$$

Now x-y coordinates are defined in the plane constructed **N** and **B**, and the axial directions of x and y are coinciding with **N** and **B**, respectively, so that the position vector of a general point in space can be represented by

$$\mathbf{r} = \mathbf{R} + x\mathbf{N} + y\mathbf{B}, \tag{4}$$

Here, the natural base vectors $(\mathbf{e}_x, \mathbf{e}_y, \mathbf{e}_z)$, which corresponding to coordinates *(x,y,z)*, are non-orthogonal, whereas, the physical base vectors $(\mathbf{N}, \mathbf{B}, \mathbf{T})$ are orthogonal, and the relationship between these two coordinate systems is

$$\begin{pmatrix} \mathbf{e}_x \\ \mathbf{e}_y \\ \mathbf{e}_z \end{pmatrix} = \begin{pmatrix} 1 & 0 & 0 \\ 0 & 1 & 0 \\ -\tau y & -\tau x & m \end{pmatrix} \begin{pmatrix} \mathbf{N} \\ \mathbf{B} \\ \mathbf{T} \end{pmatrix}, \quad m = 1 - kx \tag{5}$$

Thus the metric tensors are

$$\left[G_{ij}\right] = \begin{pmatrix} 1 & 0 & -\tau x \\ 0 & 1 & \tau x \\ -\tau y & \tau x & m^2 + \tau^2\left(x^2 + y^2\right) \end{pmatrix}, \tag{6}$$

and non-zero Christoffel symbols are

$$\Gamma_{13}^1=\Gamma_{31}^1=-\frac{k\tau y}{m},\quad \Gamma_{23}^1=\Gamma_{32}^1=-\tau \qquad \Gamma_{33}^1=km-\tau^2x+\frac{k\tau^2y^2}{m}-M_1$$

$$\Gamma_{13}^2=\Gamma_{31}^2=\frac{\tau}{m} \qquad \Gamma_{33}^2=-\frac{\tau^2y}{m}+M_2,\quad \Gamma_{13}^3=\Gamma_{31}^3=-\frac{k}{m},\quad \Gamma_{33}^2=\frac{k\tau y}{m}-M_3, \tag{7}$$

$$M_1=k'\frac{\tau xy}{m}+\tau' y \quad M_2=k'\frac{\tau x^2}{m}+\tau' x,\quad M_3=k'\frac{x}{m}.$$

Here and later k', τ' denote the derivative with respect to s.

After further standard tensor operation refer to Ref. [13], we obtain following basic equations in a curvilinear orthogonal system continuity equation

$$\frac{\partial u}{\partial x}+\frac{\partial v}{\partial y}+\frac{\tau y}{m}\frac{\partial w}{\partial x}-\frac{\tau x}{m}\frac{\partial w}{\partial y}+\frac{1}{m}\frac{\partial w}{\partial s}-\frac{k}{m}u=0, \tag{8}$$

Navier-Strokes equations

$$\frac{\partial u}{\partial t}+u\frac{\partial u}{\partial x}+v\frac{\partial u}{\partial y}+\frac{w}{m}\left(\tau y\frac{\partial u}{\partial x}-\tau x\frac{\partial u}{\partial y}+\frac{\partial u}{\partial s}-\tau v+kw\right)=-\frac{1}{\rho}\frac{\partial p}{\partial x}+\nu\left(\nabla^2\mathbf{V}\right)^{(1)}, \tag{9}$$

$$\frac{\partial v}{\partial t}+u\frac{\partial v}{\partial x}+v\frac{\partial v}{\partial y}+\frac{w}{m}\left(\tau y\frac{\partial v}{\partial x}-\tau x\frac{\partial v}{\partial y}+\frac{\partial v}{\partial s}+\tau u\right)=-\frac{1}{\rho}\frac{\partial p}{\partial y}+\nu\left(\nabla^2\mathbf{V}\right)^{(2)}, \tag{10}$$

$$\begin{aligned}\frac{\partial w}{\partial t}+u\frac{\partial w}{\partial x}+v\frac{\partial w}{\partial y}+\frac{w}{m}\left(\tau y\frac{\partial w}{\partial x}-\tau x\frac{\partial w}{\partial y}+\frac{\partial w}{\partial s}-ku\right)=\\ -\frac{1}{\rho m}\left(\tau y\frac{\partial p}{\partial x}-\tau x\frac{\partial p}{\partial y}+\frac{\partial p}{\partial s}\right)+\nu\left(\nabla^2\mathbf{V}\right)^{(3)},\end{aligned} \tag{11}$$

where

$$\begin{aligned}\left(\nabla^2\mathbf{V}\right)^{(1)}=\frac{1}{m^2}\Big[&\left(m^2+\tau^2y^2\right)\frac{\partial^2u}{\partial x^2}+\left(m^2+\tau^2x^2\right)\frac{\partial^2u}{\partial y^2}+\frac{\partial^2u}{\partial s^2}-2\tau^2xy\frac{\partial^2u}{\partial x\partial y}+2\tau y\frac{\partial^2u}{\partial x\partial s}\\ &-2\tau x\frac{\partial^2u}{\partial y\partial s}+A\frac{\partial u}{\partial x}-B\frac{\partial u}{\partial y}+C\frac{\partial u}{\partial s}-2\tau^2y\frac{\partial v}{\partial x}+2\tau^2x\frac{\partial v}{\partial y}-2\tau\frac{\partial v}{\partial s}+2k\tau y\frac{\partial w}{\partial x}\\ &-2k\tau x\frac{\partial w}{\partial y}+2k\frac{\partial w}{\partial s}-(k^2+\tau^2)u-Dv+Ew\Big],\end{aligned} \tag{12}$$

$$\begin{aligned}\left(\nabla^2\mathbf{V}\right)^{(2)}=\frac{1}{m^2}\Big[&\left(m^2+\tau^2y^2\right)\frac{\partial^2v}{\partial x^2}+\left(m^2+\tau^2x^2\right)\frac{\partial^2v}{\partial y^2}+\frac{\partial^2v}{\partial s^2}-2\tau^2xy\frac{\partial^2v}{\partial x\partial y}+2\tau y\frac{\partial^2v}{\partial x\partial s}\\ &-2\tau x\frac{\partial^2v}{\partial y\partial s}+2\tau^2y\frac{\partial u}{\partial x}-2\tau^2x\frac{\partial u}{\partial y}+2\tau\frac{\partial u}{\partial s}+A\frac{\partial v}{\partial x}-B\frac{\partial v}{\partial y}+C\frac{\partial v}{\partial s}+Du-\tau^2v+k\tau w\Big]\end{aligned} \tag{13}$$

$$\begin{aligned}\left(\nabla^2\mathbf{V}\right)^{(3)}=\frac{1}{m^2}\Big[&\left(m^2+\tau^2y^2\right)\frac{\partial^2w}{\partial x^2}+\left(m^2+\tau^2x^2\right)\frac{\partial^2w}{\partial y^2}+\frac{\partial^2w}{\partial s^2}-2\tau^2xy\frac{\partial^2w}{\partial x\partial y}+2\tau y\frac{\partial^2w}{\partial x\partial s}\\ &-2\tau x\frac{\partial^2w}{\partial y\partial s}-2k\tau y\frac{\partial u}{\partial x}+2k\tau x\frac{\partial u}{\partial y}-2k\frac{\partial u}{\partial s}+A\frac{\partial w}{\partial x}-B\frac{\partial w}{\partial y}+C\frac{\partial w}{\partial s}-Eu+k\tau v-k^2w\Big]\end{aligned} \tag{14}$$

and

$$A=\frac{k\tau^2y^2}{m}-\tau^2x-km+M_1,\quad B=\frac{\tau^2y}{m}+M_2,\quad C=\frac{k\tau y}{m}+M_3,$$
$$D=\frac{k\tau^2y}{m}+\tau'+\tau M_3,\qquad E=\frac{k^2\tau y}{m}+k'+kM_3. \tag{15}$$

3. Geometry of helical pipe

A helical pipe is constructed by winding a pipe of radius R around a cylinder of radius (r_a-R) (see Fig. 2). With the pitch p_s, defined by the increase in elevation per revolution of coils $h_g=2\pi p_s$, the curvature k and torsion τ of the helical pipe axis can be calculated from

$$k=\frac{r_a}{\left(r_a^2+p_s^2\right)},\qquad \text{and}\quad \tau=\frac{p_s}{\left(r_a^2+p_s^2\right)}.$$

The curvature and torsion of centerline of the pipe are all constants. So the partial derivatives of parameters k and τ with respect to s are all equal to zero. Obviously if torsion τ is zero, the pipe is the same as the planar curved pipe studied by Dean.

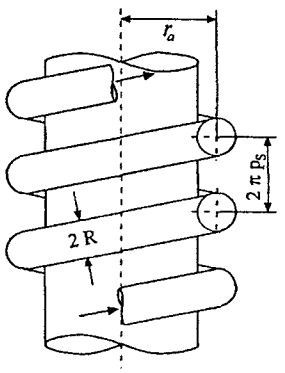

Fig. 2. Helical coiled pipe

4. Equations of the laminar flow in a helical pipe.

4.1 Equations of steady fully developed laminar flow.

Secondary flow is the main phenomenon studied in curved pipes. Because turbulence itself is very complex, so far it is still difficult to predict the disciplinarian of turbulent secondary flow in curved pipes according to Ref. [14]. However, the problem of laminar flow is relatively simple, and its analysis might directly reveal the mechanism of the secondary flow. So, we thought it wise to confine this research within the range of laminar flow. Because of the influence of k and τ, the turbulent transition point will be raised, as reported in Ref. [15]. In other words, many practical engineering applications may be in the field of the laminar flow.

Now we make the following assumptions:

(1) the flow is steady and laminar;

(2) the end effects are ignored and the fluid flow in the pipe is fully developed so that

$$\frac{\partial}{\partial t}=0, \qquad \frac{\partial \mathbf{V}}{\partial s}=0, \qquad p(x,y,s)=cs+p_0(x,y), \tag{16}$$

where the axial pressure gradient $c=(\partial p/\partial s)$ is constant.

In order to render the governing equations dimensionless, all lengths are referred to radius R. So

$$x=R\bar{x}, \quad y=R\bar{y}, \quad s=R\bar{s}, \quad \bar{k}=Rk, \quad \bar{\tau}=R\tau, \tag{17}$$

and the dimensionless expressions of velocity and pressure are

$$(\bar{u},\bar{v},\bar{w})=\left(\frac{u}{U},\frac{v}{U},\frac{w}{U}\right), \quad \bar{p}=\frac{p}{\rho}\left(\frac{R}{v}\right)^2, \tag{18}$$

where a velocity scale is defined by

$$U=-\frac{dp}{ds}\cdot\frac{R^2}{4\mu}$$

Based on it, we have Reynolds number $\mathrm{Re}=UR/\nu$ (for the reason of simplicity, the superscript "-" is omitted and variables appearing later are all dimensionless) and Dean number $K=2k(\mathrm{Re})^2$. Since the axial velocity component w is perpendicular to (x,y) plane, and to find the global property of a helical pipe, we define the flow ratio as

$$\lambda_Q=\frac{Q}{Q_s}=\frac{\int_\Omega \bar{w}d\Omega}{\int_\Omega \bar{w}_s d\Omega}$$

where Ω is the area of the cross-section and Q denotes the flux in a helical pipe and Q_s the flux in a straight pipe for the same pressure gradient as that in a helical pipe. Analogous to Masliyah [8], the stream function ψ, which satisfies the continuity equation, is defined as

$$u=\frac{1}{m}\left(\frac{\partial\psi}{\partial y}-\tau yw\right), \qquad v=-\frac{1}{m}\left(\frac{\partial\psi}{\partial x}-\tau xw\right). \tag{20}$$

Substituting Eq. (20) into Navier-Stokes equations and eliminating the pressure terms, the following equations are obtained (where the subscripts denote derivatives)

$$\left\{f\left(\frac{1}{m}\psi_y\right)+\left[yf\left(-\frac{\tau w}{m}\right)+\frac{2\tau w}{m^2}\psi_x\right]+w^2\left(\frac{k}{m}-\frac{\tau^2 x}{m^2}\right)-\left(\nabla^2\mathbf{V}\right)^{(1)}\right\}_y$$
$$=\left\{f\left(-\frac{1}{m}\psi_x\right)+\left[xf\left(\frac{\tau w}{m}\right)+\frac{2\tau w}{m^2}\psi_y\right]-\frac{\tau^2 y}{m^2}w^2-\left(\nabla^2\mathbf{V}\right)^{(2)}\right\}_x, \tag{21}$$

$$-\tau y f\left(\frac{1}{m}\psi_y\right)-\tau x f\left(\frac{1}{m}\psi_x\right)+\tau^2\left(x^2+y^2\right)f\left(\frac{w}{m}\right)+\frac{2\tau^2}{m^2}\left(xw\psi_y-yw\psi_x\right)+$$
$$+\left[mf(w)-\frac{kw}{m}\psi_y\right]=4\,\mathrm{Re}+m\left(\nabla^2\mathbf{V}\right)^{(3)}-\tau y\left(\nabla^2\mathbf{V}\right)^{(1)}+\tau x\left(\nabla^2\mathbf{V}\right)^{(2)}, \tag{22}$$

where the operator

$$f=\frac{1}{m}\left(\psi_y\frac{\partial}{\partial x}-\psi_x\frac{\partial}{\partial y}\right).$$

According to above analysis result the problem becomes how to get the solutions of the stream function ψ and the axial velocity component w under the wall boundary conditions

$$\psi=0,\ \frac{\partial\psi}{\partial n}=0,\ \ w=0, \tag{23}$$

where n is the independent variable along the direction of the inner normal of the wall boundary.

4.2 Governing equations of unsteady flow.

As suggested by Germano [7], an orthogonal helical coordinate system is introduced with respect to a master Cartesian coordinate system (x_1,x_2,x_3). By using the helical coordinate s for axial direction, r for radial direction and θ for the circumferential direction, the position of any given point X inside the helical pipe can be described by the vector $\vec{x}$

$$\vec{x}=\vec{P}(s)-r\sin(\theta-\tau s)\vec{N}(s)+r\cos(\theta-\tau s)\vec{B}(s)$$

Here $\vec{T},\vec{N}$, and $\vec{B}$ are the tangential, normal and binormal directions to the generic curve of the helical pipe axis, $\vec{P}(s)$ at the point of consideration (see Fig. 3.)

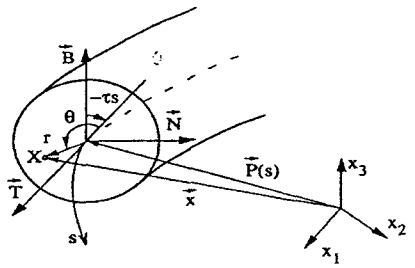

Fig.3. Description of the orthogonal helical (s,r,θ) - coordinate system, as introdused by Germano (1982, 1989)

The metric of the orthogonal helical coordinate system is given by

$$d\vec{x}\cdot d\vec{x}=(1+kr\sin(\theta-\tau s))^2ds^2+dr^2+r^2d\theta^2 \tag{24}$$

where ds, dr, and $d\theta$ are the infinitesimal increments in the axial, radial, and circumferential directions. With this metric one obtains the scale factors h_s, h_r, and h_θ

$$h_r = 1 + kr\sin(\theta - \tau s), \quad h_r = 1, \quad h_\theta = r. \tag{25}$$

The incompressible Navier-Stokes equations, expressed in these orthogonal helical coordinates read in non-dimensional form:

(a) Continuity equation

$$\frac{\partial}{\partial s}(ru_s) + \frac{\partial}{\partial r}(h_s ru_r) + \frac{\partial}{\partial \theta}(h_s u_\theta) = 0. \tag{26}$$

(b) s-momentum equation:

$$\begin{aligned}
&\frac{\partial u_s}{\partial t} + \frac{1}{h_s}\frac{\partial}{\partial s}(u_s u_s) + \frac{1}{h_s r}\frac{\partial}{\partial r}(h_s r u_s u_r) + \frac{1}{h_s r}\frac{\partial}{\partial \theta}(h_s u_s u_\theta) + \\
&+ \frac{k\sin(\theta - \tau s)}{h_s} u_s u_r + \frac{k\sin(\theta - \tau s)}{h_s} u_s u_\theta = \\
&= -\frac{1}{h_s}\frac{\partial p}{\partial s} + \frac{1}{\mathrm{Re}_\tau}\left[\frac{2}{h_s}\frac{\partial}{\partial s}\left(\frac{1}{h_s}\left(\frac{\partial u_s}{\partial s} + k\sin(\theta - \tau s)u_r + \right.\right.\right. \\
&\left.\left.\left. + k\cos(\theta - \tau s)u_\theta\right)\right) + \frac{1}{h_s r}\frac{\partial}{\partial r}\left(h_s h_s r\frac{\partial}{\partial r}\left(\frac{u_s}{h_s}\right) + r\frac{\partial u_r}{\partial s}\right) + \right. \\
&+ \frac{1}{h_s r}\frac{\partial}{\partial \theta}\left(\frac{h_s h_s}{r}\frac{\partial}{\partial \theta}\left(\frac{u_s}{h_s}\right) + \frac{\partial u_r}{\partial s}\right) + \\
&+ k\sin(\theta - \tau s)\left(\frac{\partial}{\partial r}\left(\frac{u_s}{h_s}\right) + \frac{1}{h_s h_s}\frac{\partial u_r}{\partial s}\right) + \\
&\left. + k\cos(\theta - \tau s)\left(\frac{1}{r}\frac{\partial}{\partial \theta}\left(\frac{u_s}{h_s}\right) + \frac{1}{h_s h_s}\frac{\partial u_\theta}{\partial s}\right)\right],
\end{aligned} \tag{27}$$

(c) r-momentum equation:

$$\begin{aligned}
&\frac{\partial u_r}{\partial t}+\frac{1}{h_s}\frac{\partial}{\partial s}(u_s u_r)+\frac{1}{h_s r}\frac{\partial}{\partial r}(h_s r u_r u_r)+\frac{1}{h_s r}\frac{\partial}{\partial \theta}(h_s u_r u_\theta)- \\
&-\frac{k\sin(\theta-\tau s)}{h_s}u_s u_s-\frac{u_\theta u_\theta}{r}= \\
&=-\frac{\partial p}{\partial r}+\frac{1}{\mathrm{Re}_\tau}\left[\frac{1}{h_s}\frac{\partial}{\partial s}\left(h_s\frac{\partial_s}{\partial r}\left(\frac{u_s}{h_s}\right)+\frac{1}{h_s}\frac{\partial u_r}{\partial s}\right)+\right. \\
&+\frac{2}{h_s r}\frac{\partial}{\partial r}\left(h_s r\frac{\partial u_r}{\partial r}\right)+\frac{1}{h_s}\frac{\partial}{\partial \theta}\left(h_s\left(\frac{1}{rr}\frac{\partial u_r}{\partial \theta}+\frac{\partial}{\partial r}\left(\frac{u_\theta}{r}\right)\right)\right)- \\
&-\frac{2k\sin(\theta-\tau s)}{h_s h_s}\left(\frac{\partial u_s}{\partial s}+k\sin(\theta-\tau s)u_r+\right. \\
&\left.\left.+k\cos(\theta-\tau s)u_\theta\right)-\frac{2}{rr}\left(\frac{\partial u_\theta}{\partial \theta}+u_r\right)\right],
\end{aligned} \tag{28}$$

(d) θ momentum equation

$$\begin{aligned}
&\frac{\partial u_\theta}{\partial t}+\frac{1}{h_s}\frac{\partial}{\partial s}(u_s u_\theta)+\frac{1}{h_s r}\frac{\partial}{\partial r}(h_s r u_r u_\theta)+\frac{1}{h_s r}\frac{\partial}{\partial \theta}(h_s u_\theta u_\theta)- \\
&-\frac{k\cos(\theta-\tau s)}{h_s}u_s u_s+\frac{u_r u_\theta}{r}= \\
&=-\frac{1}{r}\frac{\partial p}{\partial \theta}+\frac{1}{\mathrm{Re}}\left[\frac{1}{h_s}\frac{\partial}{\partial s}\left(\frac{h_s}{r}\frac{\partial}{\partial \theta}\left(\frac{u_s}{h_s}\right)+\frac{1}{h_s}\frac{\partial u_\theta}{\partial s}\right)+\right. \\
&+\frac{1}{h_s r}\frac{\partial}{\partial r}\left(h_s\left(\frac{\partial u_r}{\partial \theta}+rr\frac{\partial}{\partial r}(\frac{u_\theta}{r})\right)\right)+ \\
&+\frac{2}{h_s rr}\frac{\partial}{\partial \theta}\left(h_s\left(\frac{\partial u_\theta}{\partial \theta}+u_r\right)\right)- \\
&-\frac{2k\cos(\theta-\tau s)}{h_s h_s}\left(\frac{\partial u_s}{\partial s}+k\sin(\theta-\tau s)u_r+\right. \\
&\left.\left.+k\cos(\theta-\tau s)u_\theta\right)+\left(\frac{1}{rr}\frac{\partial u_r}{\partial \theta}+\frac{\partial}{\partial r}\left(\frac{u_\theta}{r}\right)\right)\right],
\end{aligned} \tag{29}$$

The pipe radius R has been used to non-dimensionalize coordinates and scale factors. The mean friction velocity u_τ and R/u_τ are proper velocity and time scales. The dimensionless mass density is set to 1. The mean friction velocity is defined as the square root of the wall shear stress averaged over the circumference:

$$u_\tau=\sqrt{\frac{\tau_{w,m}}{\rho}},\quad \text{with } \tau_{w,m}=\frac{1}{2\pi}\int_{\theta=0}^{2\pi}\tau_w(\theta)\,d\theta \tag{30}$$

The dimensionless curvature k and torsion τ are scaled by the pipe radius R.
The Reynolds, Dean and Germano numbers based on these scaling quantities are:

$$\mathrm{Re}_\tau = \frac{Ru_\tau}{\nu}, \quad De = \sqrt{k}\,\mathrm{Re}, \quad Gn = \tau\,\mathrm{Re} \tag{31}$$

The Reynolds number . • represents the ration of inertia and viscous forces. The Dean and Germano numbers represent the ratio of the product of the inertia and centrifugal forces to the viscous forces.

5. On analytical and approximate solutions

Many investigations have been conducted regarding fluid flow in curved and helicoidal pipes with circular cross sections. One of the principal features of the fluid flows in a helical pipe is the occurrence of a secondary flow in planes normal to the main flow, which causes the momentum and energy transport in the curved pipe to be substantially different from that of the flow in a straight pipe and dramatically increases the difficulty of theoretical analysis of the physical problem in a helical pipe.

The first theoretical study on the flow of a Newtonian fluid in a curved pipe was made by Dean [19,20], who found the dependence of dynamic similarity of the fully developed flow on a nondimensional parameter

$$D = \left[\frac{a}{R}\cdot\frac{2a^2W_0^2}{\nu^2}\right]^{1/2}$$

where W_0 is the mean velocity along the pipe, ν the kinematics viscosity, and a the radius of the pipe, which is bent in a circle of radius R. Dean studied the problem by perturbing the solution with respect to small Dean number *(D)* on the basis of Poiseuille's flow.

The curved pipe has pitch if it is bent more than one turn. The helical pipe with pitch has been used extensively in various industrial applications to enhance the rate of heat, mass and momentum transfer. In order to improve the performance of these devices, an accurate and reliable analysis of the flow in the helical pipe is necessary. The flow in the helical pipe has been studied for circular (Wang, 1981 [6]; Murata et al., 1981 [5]; Germano, 1982 [7]; Chen and Fan, 1986 [21]; Kao, 1987 [9]; Xie, 1990 [22]; Tuttle, 1990 [10]; Chen and Jan, 1992 [11]) and elliptical (Germano, 1989 [18]) cross-sections. The previous theoretical studies of the helical pipe flow mentioned above are limited to small curvature and torsion.

Liu and Masliyah (1993 [23]) numerically solved the problem of laminar flows in a circular pipe having a non-zero pitch. They discussed in detail secondary flow patterns in a cross-section of the pipe. However, their analysis is limited to small Dean number and small curvature. Yamamoto et al. (1994 [24]) investigated numerically the flow through a helical pipe for a wide range of the Dean number, curvature and torsion. They employed the orthogonal coordinate system and solved the equations numerically by applying the spectral method. Yamamoto et al. (1995 [25]) also conducted experiments

on the flow in helical circular tube over a range of Reynolds numbers from about 500 to 2000. The results reveal rather a large effect of torsion on the flow.

5.1 **Analytical approximate solution.**

In the literature, the commonly used methods are theoretical analysis and numerical discretization. It is known that the analytical techniques have the major advantage over numerical discretization techniques of providing physical insight into the nature of the solution of the problem. Perturbation technique, as an approximately theoretical analytical technique, is the most important method used in this field. Despite its usefulness, perturbation technique also has two major drawbacks. Firstly, for practical applications, the perturbation series has to be restricted to a few terms; secondly, in order to obtain solutions of acceptable accuracy, the perturbation parameters are limited to be small. And as one of the methods of weighted residuals, Galerkin technique might overcome these limitations and obtain high-order semianalytical solutions that are unavailable by direct numerical discretization.

To obtain the solution for flow in a helical pipe, the Galerkin technique is adopted. The solutions of the stream function ψ and the axial velocity component w under the wall boundary conditions

$$\psi = 0, \ \frac{\partial \psi}{\partial n} = 0, \ w = 0, \tag{32}$$

where n is the independent variable along the direction of the inner normal of the wall boundary.

Firstly, the base function series $\{\psi_i\}$ and $\{w_j\}$, $(i, j = 1,2,\ldots)$ are chosen, ψ and w are expressed as

$$\psi = \sum_{i=1}^{n_1} c_i \psi_i, \quad w = \sum_{j=1}^{n_2} b_j w_j, \tag{33}$$

where n_1, n_2 denote the numbers of the terms in series $\{\psi_i\}$ and $\{w_i\}$.

In order to satisfy the boundary conditions (32), ψ_i, w_j are simply given as follows:

$$\psi_i = \left[1-(x^2+y^2)\right]^2 \psi_{0i}, \ \ w_j = \left[1-(x^2+y^2)\right]^2 w_{0j}$$

where the series $\{\psi_{0i}\}$, $\{w_{0j}\}$, $(i, j = 1,2,\ldots)$ can be selected from linear irrelative power series as $\{x^i y^j\}$, $(i, j = 1,2,\ldots)$.

Secondly, substituting Eq. (33) into Eqs. (21) and (22) and integrating them by Galerkin criterion, we can obtain a set of equations concerning those coefficients b_j, c_i . Solutions of b_j, c_i are listed below for different dimensionless values of k, τ and Re provided they are replaced by Eq. (33).

Using this data we can immediately obtain corresponding approximate semianalytical solutions.

The solutions for the helical circular pipes with different parameters of k and τ . cs is the coefficients of base functions ψ_i and cw is the coefficients of base functions w_j.

Planar curved pipes

The selected base functions are

$\{y, x\cdot y, x^2\cdot y, y^3, x^3\cdot y, x\cdot y^3, x^4\cdot y, x^2\cdot y^3, y^5, x^5\cdot y,$
$x^3\cdot y^3, x\cdot y^5, x^6\cdot y, x^4\cdot y^3, x^2\cdot y^5, y^7, x^7\cdot y, x^5\cdot y^3,$
$x^3\cdot y^5, x\cdot y^7, x^8\cdot y, x^6\cdot y^3, x^4\cdot y^5, x^2\cdot y^7, y^9, x^9\cdot y, x^7\cdot y^3, x^5\cdot y^5, x^3\cdot y^7, x\cdot y^9\}$

for ψ_i and

$\{1, x, x^2, y^2, x^3, x\cdot y^2,$
$x^4, x^2\cdot y^2, y^4, x^5, x^3\cdot y^2, x\cdot y^4, x^6, x^4\cdot y^2, x^2\cdot y^4,$
$y^6, x^7, x^5\cdot y^2, x^3\cdot y^4, x\cdot y^6, x^8, x^6\cdot y^2, x^4\cdot y^4,$
$x^2\cdot y^6, y^8, x^9, x^7\cdot y^2, x^5\cdot y^4, x^3\cdot y^6, x\cdot y^8, x^{10},$
$x^8\cdot y^2, x^6\cdot y^4, x^4\cdot y^6, x^2\cdot y^8, y^{10}, x^{11}, x^9\cdot y^2, x^7\cdot y^4,$
$x^5\cdot y^6, x^3\cdot y^8, x\cdot y^{10}\}$

for w. In some cases, the corresponding coefficients of these bases are as follows:

(1) k = 0.01, Re = 100

cs = {-0.0136011, 0.0019697, 0.00300443, 0.00318328,-0.00102175,
> -0.00103148, 0.000392012, 0.000675116, 0.000282771, 0.000183283,
> 0.000370624, 0.00018734, -0.000202783, -0.00057964, -0.000551095,
> -0.000174239, 0.0000376974, 0.000112526, 0.000111998, 0.0000371698,
> 0.0000516213, 0.000201541, 0.000295084, 0.000192032, 0.0000468674,
> -0.0000251516, -0.00010006, -0.000149294, -0.0000990126, -0.0000246278};

cw = {0.988913, -0.149107, 0.0522874, 0.330089, 0.157918, 0.159392,
> -0.0843738, -0.139312, -0.0548318, -0.0375955, -0.0781548, -0.0405668,
> 0.0663112, 0.182527, 0.165857, 0.0496409, -0.0315306, -0.0921868,
> -0.0897614, -0.0291052, -0.0261025, -0.102309, -0.150069, -0.0976206,
> -0.0237579, 0.0223779, 0.0886286, 0.131599, 0.868232, 0.0214752,
> 0.00423684, 0.0218186, 0.044825, 0.0459316, 0.0234783, 0.00478999,
> -0.00538846, -0.026822, -0.0533968, -0.0531429, -0.0264411, -0.0052615}

(2) k = 0.05, Re = 100

cs = {-0.0519733, 0.0228646, -0.00277109, 0.00169482, 0.0000669753,
> 0.000424743, 0.00794113, 0.0203529, 0.0127148, -0.0115318, -0.0268187,
> -0.0153807, 0.00190328, -0.00162642, -0.0098619, -0.00634314,
> 0.00695402, 0.0249026, 0.0291472, 0.0111999, -0.00190688, -0.00491976,
> -0.00280932, 0.00152519, 0.00132168, -0.00150356, -0.00738378,
> -0.0132318, -0.0103277, -0.00297618};

cw ={0.866075, -0.375426, 0.452664, 0.364562, 0.00903087, -0.0136394,
> -0.319629, -0.795097, -0.487978, 0.586728, 1.36388, 0.781013, -0.339092,
> -0.462905, 0.145876, 0.27027,-0.394109, -1.57918, -1.99072, -0.805711,
> 0.558184, 1.74223, 1.80367, 0.611979, -0.00763865, -0.043975, 0.161784,
> 0.767529, 0.873951, 0.312181, -0.209025, -0.901423, -1.48294, -1.1297,
> -0.371144, -0.0319878, 0.0729989, 0.259752, 0.301475, 0.0758221,
> -0.0787673, -0.0398675}

(3) k = 0.05, Re = 500

cs = {-0.0333715, -0.00757938, -0.00494806, -0.0493697, 0.0362666,
> -0.0121968, -0.044979, -0.0501575, -0.0635308, 0.0847873, 0.366537,
> 0.21519, -0.016949, -0.0258582, 0.0965767, 0.0839798, -0.10495,
> -0.536138, -0.581609, -0.162041, 0.0371521, 0.1204, 0.0893902,
> -0.00792362, -0.0169364, 0.0281796, 0.19893, 0.314676, 0.162044,
> 0.0178938};

cw = {0.465881, -0.265519, 0.541209, 0.775909, -0.366097, -0.103976,
> 0.0767799, -0.109164, 0.842459, -0.134997, -2.9027, -1.33759, 1.8523,
> 4.9397, 1.98518, -0.711493, -0.873688, 2.11391, 1.16305, -1.48754,
> -3.75298, -13.8821, -17.3538, -8.85126, -1.61037, 2.9674, 8.64339,
> 15.401, 15.9776, 6.21148, 1.77433, 8.3943, 15.4159, 14.0451, 6.51412,
> 1.27098, -1.67919, -7.63398, -16.8003, -20.9455, -13.5947, -3.49393}

(4) k = 0.5, Re = 20

cs = {-0.11191, 0.00592478, 0.0232902, 0.0233443, -0.00572275, -0.00583517,
> 0.00442198, 0.0044002, 0.0000497176, 0.00395448, 0.00524411, 0.00129413,
> -0.00192894, -0.00399484, -0.000839882, 0.00112813, -0.000386158,
> 0.000268643, 0.00242005, 0.0017349, 0.000996813, 0.00364289, 0.00436538,
> 0.00170063, 6.29611 * 10^{A} - 6, 0.00192592, 0.00056755, 0.000182284,
> -0.000619558, -0.000417892};

cw ={0.90193, 0.0889081, 0.142641, 0.201261, 0.3034, 0.38609, -0.00444416,
> -0.19691, -0.263529, -0.0589189, -0.289219, -0.2832, 0.109447, 0.267758,
> 0.320385, 0.194324, 0.00993847, 0.0421307, 0.148575, 0.136541,
> -0.0623018, -0.215673, -0.269702, -0.192244, -0.0823239, -0.000849267,
> 0.0162203, 0.0165683, -0.0450485, -0.0498734, 0.010763, 0.0535704,
> 0.0961453, 0.0840662, 0.0484134, 0.0176455, -0.00296688, -0.0159449,
> -0.0325528, -0.0229767, 0.0070944, 0.0105755}

The selected base functions are

$\{1, x, y, x^2, x\cdot y, y^2, x^3, x^2\cdot y, x\cdot y^2, y^3, x^4, x^3\cdot y, x^2\cdot y^2,$
$x\cdot y^3, y^4, x^5, x^4\cdot y, x^3\cdot y^2, x^2\cdot y^3, x\cdot y^4, y_5, x^6, x^5\cdot y, x^4\cdot y^2, x^3\cdot y^3, x^2\cdot y^4, x\cdot y^5,$
$y^6, x^7, x^6\cdot y, x^5\cdot y^2, x^4\cdot y^3, x^3\cdot y^4, x^2\cdot y^5, x\cdot y^6, y^7, x^8, x^7\cdot y, x^6\cdot y^2, x^5\cdot y^3,$
$x^4\cdot y^4, x^3\cdot y^5, x^2\cdot y^6, x\cdot y^7, y^8\}$

for ψ and

$\{1, x, y, x^2, x\cdot y, y^2, x^3, x^2\cdot y, x\cdot y^2, y^3, x^4, x^3\cdot y,$
$x^2\cdot y^2, x\cdot y^3, y^4, x^5, x^4\cdot y, x^3\cdot y^2, x^2\cdot y^3, x\cdot y^4, y^5,$
$x^6, x^5\cdot y, x^4\cdot y^2, x^3\cdot y^3, x^2\cdot y^4, x\cdot y^5, y^6, x^7, x^6\cdot y,$
$x^5\cdot y^2, x^4\cdot y^3, x^3\cdot y^4, x^2\cdot y^5, x\cdot y^6, y^7, x^8, x^7\cdot y, x^6\cdot y^2,$
$x^5\cdot y^3, x^4\cdot y^4, x^3\cdot y^5, x^2\cdot y^6, x\cdot y^7, y^8, x^9, x^8\cdot y, x^7\cdot y^2,$
$x^6\cdot y^3, x^5\cdot y^4, x^4\cdot y^5, x^3\cdot y^6, x^2\cdot y^7, x\cdot y^8, y^9,\}$

for w. In some cases, the corresponding coefficients of these bases are as follows.

(1) k = 0.05, x = 0.1, Re = 20

cs= {-0.0248882, -0.0012192, -0.0139442, -0.0000581824, 0.000123405,
> -0.000155551, 0.000436779, 0.00343005, 0.000435015, 0.00343176,
> 0.0000181083, -0.000101653, 0.0000941946, -0.000101582, 0.0000762716,
> -0.000203246, 0.0000230267, -0.000405818, 0.0000394039, -0.000202562,
> 0.0000163796, -5.65523 * E-06, 0.0000587232, -0.0000308348, 0.000117008,
> -0.0000448924, 0.000058285, -0.0000197136, 0.000028804, -5.05408 * E-06,
> 0.000086969, -0.0000120321, 0.0000875154, -8.89893 * E-06, 0.0000293505,
> -1.92088 * E-06,0, -9.17128 * E-06, 4.01345 * E-06, -0.0000272493,
> 0.0000124828, -0.0000269842, 0.0000126507, -8.90615 * E-06, 4.25022 * E-06};

cw ={0.998675, 0.00547226, 0.00898449, 0.00211156, 0.000619652, 0.00288532,
> 0.0353207, -0.00492927, 0.0354188, -0.00497833, -0.000983888,
> -0.000324348, -0.00472752, -0.000327555, -0.00375152, -0.0148657,
> 0.00371974, -0.0299647, 0.00748802, -0.0150996, 0.00376853, 0.00140719,
> 0.00025098, 0.00527498, 0.000504944, 0.00634466, 0.000253972,
> 0.00247689, 0.00150888, -0.00160201, 0.00464065, -0.00484939,
> 0.00475594, -0.00489308, 0.00162416, -0.00164571, -0.000629338,
> -0.0000935552, -0.00254312, -0.00028199, -0.00386051, -0.000283319,
> -0.00260904, -0.0000948839, -0.00066231, 0.0000284995, 0.000271819,
> 0.000100436, 0.00110368, 0.00012969, 0.00168031, 0.0000720664,
> 0.00113686, 0.0000143135, 0.000288409}

(2) k = 0.05, 1 = 0.1, Re = 100

cs= {-0.0162417, -0.00966635, -0.052046, 0.00168474, 0.016527, -0.0147042,
> 0.00691662, -0.000904487, 0.0123034, -0.00105541, -0.00383404,
> 0.00495473, 9.71291 * E-06, 0.00572502, 0.00379442, -0.0018611,
> 0.00814212, -0.00385503, 0.021433, -0.00185773, 0.0133701, 0.00295886,

```
>      -0.0121577, 0.00810731, -0.0254303, 0.00946565, -0.0132534, 0.00434416,
>      -0.000343084, -0.000932743, -0.00256758, -0.00622004, -0.00435395,
>      -0.00963789, -0.00213082, -0.00434991, -0.000962907, 0.00465002,
>      -0.00413409, 0.0143963, -0.00802421, 0.0148052, -0.00752598, 0.00505874,
>      -0.00267296};
```

```
cw = {0.869707, -0.325366, 0.186191, 0.414993, -0.102432, 0.392156,
>      -0.019985, -0.0499992, -0.0367487, -0.0425871, -0.402434, -0.00289807,
>      -0.927729, -0.00770253, -0.52658, 0.637493, -0.155417, 1.32061,
>      -0.398444, 0.682932, -0.243669, 0.0522123, 0.182941, 0.420724, 0.379812,
>      0.68559, 0.196914, 0.317007, -0.57487, 0.138895, -1.7726, 0.5579,
>      -1.81983, 0.700424, -0.622105, 0.281417, 0.0659776, -0.113865, 0.129408,
>      -0.351037, -0.00750136, -0.360521, -0.139239, -0.123348, -0.0683068,
>      0.159774, -0.0298619, 0.656116, -0.184845, 1.00916, -0.3760555, 0.689072,
>      -0.317022, 0.176253, -0.0959496}
```

(3) k = 0.5, x = 0.1, Re = 20

```
cs= {-0.0167545, -0.0104463, -0.112288, -0.00530582, 0.00434975, -0.011363,
>      0.00128365, 0.222171, -0.000883376, 0.227457, 0.00105446, -0.00572929,
>      0.0055799, -0.0054761, 0.00625028, -0.00138491, 0.00427007, -0.0015075,
>      0.00450759, 0.000875696, 0.000364372, -0.000709087, 0.00460373,
>      -0.00189821, 0.00666046, -0.00285664, 0.00196665, -0.00226174,
>      0.000127661, -0.000688699, 0.00109812, -0.000720591, 0.000834093,
>      0.00115119, -0.000212494, 0.00109608, 0.0000641834, -0.000803243,
>      0.000719949, -0.00127172, 0.00131354, -0.000249292, 0.00119648,
>      0.000712071, 0.000635205};
>
```

```
cw= {0.900765, 0.0921124, 0.0579251, 0.1435, 0.0467995, 0.200797, 0.30364,
>      0.029574, 0.385369, -0.00646557, -0.00419899, 0.0153569, -0.18939,
>      -0.0104511, -0.25255, -0.0745913, -0.00894663, -0.3123, -0.0318029,
>      -0.283795, -0.00606903, 0.0992918, -0.00555632, 0.237286, -0.00794405,
>      0.280943, 0.00648977, 0.164031, 0.0381854, 0.0109535, 0.126583,
>      0.0374812, 0207501, 0.0410834, 0.131484, 0.00932264, -0.0441174,
>      0.00314239, -0.14157, 0.00514204, -0.169204, 0.000650195, -0.114734,
>      -0.00312935, -0.0437959, -0.0186071, -0.00283599, -0.0635889,
>      -0.0158574, -0.0909627, -0.0282521, -0.0784728, -0.0198661, -0.0334223,
>      -0.00389483}
```

(4) k = 0.5, 1 = 0.1, Re = 100

```
cs = {0.00233357, -0.0137179, -0.120275, -0.00547251, 0.0218337, -0.0123663,
>      0.00192338, -0.0487675, -0.0230827, -0.126464, -0.00297668, 0.1308,
>      -0.0321586, 0.106227, -0.0275854, 0.00485175, -0.053651, 0.0427915,
>      -0.000279989, 0.0349278, 0.0608826, 0.00748365, -0.145917, 0.0535403,
```

```
>      -0.238862, 0.0683199, -0.0801644, 0.0240166, -0.00616753, 0.0764526,
>      -0.0301009, 0.161127, -0.0416005, 0.0922389, -0.0164132, 0.0057535,
>      -0.00624541, 0.0648743, -0.0318375, 0.157217, -0.0504068, 0.110566,
>      -0.0290492, 0.0161888, -0.00530173};

cw = {0.519391, -0.130914, -0.0179296, 0.461915, 0.0723412, 0.932946,
>      -0.275051, 0.212005, 0.0124242, 0.20466, 0.596823, -0.0666406, 0.468797,
>      0.016528, -0.197056, 0.821136, -0.0721033, 1.00405, 0.0421431, 0.144646,
>      0.0244597, -1.52666, 0.0533458, -3.93912, 0.0280879, -3.21548,
>      -0.0937243, -0.850821, -0.476177, -0.0858593, -0.75759, -0.511484,
>      0.0798708, -0.731707, 0.293368, -0.244488, 0.917343, -0.010026, 3.19174,
>      -0.00943223, 4.18632, 0.0513861, 2.41267, 0.0660606, 0.537111, 0.202769,
>      0.0610178, 0.407293, 0.339838, -0.0300465, 0.668582, -0.473654,
>      0.531278, -0.216056, 0.13069}
```

These semi-analytical solutions can be used to test numerical algorithm to study flow in curved pipes.

5.2 Experimental data.

Here we demonstrate the experimental data of Yamamoto [25]. These data can be useful to test numerical algorithm to find approximate solution of flow through the helical tube.

Description of experimental data

Fig. 4 shows a schematic diagram of the laboratory experiment. The helical tube is made of a vinyl tube reinforced by a steel wire. The tube is wound inside the acrylic straight circular pipe. Table 1 shows the dimensions of test section employed in the experiment, i.e., the diameter $2a$ and the pitch $2\pi b$

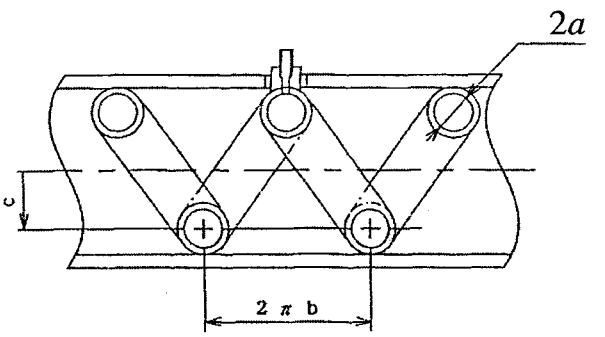

Fig. 4. Arrangements of test section of helical tube.

of the helical vinyl tube, and the distance c between the centers line of the acrylic pipe and the center of the helical vinyl tube. The lengths of the test section are about 800 mm for GC, FC and EC tubes and 1600 mm for other tubes. The non-dimensional curvature δ, the non-dimensional torsion τ, and the torsion parameter β_0 defined by

$$\delta = \frac{ac}{b^2 + c^2}, \quad \tau = \frac{ab}{b^2 + c^2}, \quad \beta_0 = \frac{\tau_0}{\sqrt{2\delta}}$$

are also shown in Table 1. The diameter of the helical tube was obtained by putting water inside and measuring its total volume together with length along the tube. The parameter δ_0 is the so-called representative curvature and is considered for three cases, δ_0 = 0.01, 0.05 and 0.1. The torsion parameter β_0 is taken for seven cases by changing it from 0.45 to 1.72. Each corresponding tube has almost the same β_0.

Table 1. Dimensions of helical tubes

Label	c (mm)	$2a$ (ram)	b (rnm)	δ	τ	β_0
(a) $\delta_0 = 0.01$						
GA	1.00	11.80	24.47	0.0098	0.241	1.72
GB	1.50	15.21	33.51	0.0101	0.226	1.59
GC	1.50	8.50	25.94	0.0094	0.163	1.19
GD	3.00	15.24	47.34	0.0102	0.160	1.12
GE	2.50	8.68	33.45	0.0096	0.129	0.93
GF	5.00	11.81	54.54	0.0098	0.107	0.77
GG	15.00	15.19	105.00	0.0101	0.071	0.50
(b) $\delta_0 = 0.05$						
FA	1.00	11.81	10.91	0.0492	0.537	1.71
FB	1.50	15.43	14.93	0.0514	0.512	1.60
FC	1.50	8.54	11.52	0.0475	0.364	1.18
FD	3.00	15.16	21.00	0.0505	0.354	1.11
FE	2.50	8.79	14.79	0.0488	0.289	0.92
FF	5.00	11.93	23.98	0.0497	0.238	0.76
FG	15.00	15.38	45.00	0.0513	0.154	0.48
(c) $\delta_0 = 0.1$						
EA	1.00	11.81	7.68	0.0984	0.756	1.70
EB	1.50	15.18	10.50	0.1012	0.708	1.57
EC	1.50	8.53	8.08	0.0947	0.510	1.17
ED	3.00	15.35	14.70	0.1023	0.501	1.11
EE	2.50	8.68	10.31	0.0964	0.398	0.91
EF	5.00	11.84	16.58	0.0987	0.327	0.74
EG	15.00	15.26	30.00	0.1017	0.203	0,45

Definition of friction factor

The pressure inside the helical tube may vary along the circumferential direction as well as the axial direction of the tube. A line on which the helical tube touches the inside of the acrylic straight pipe is helical and may be called a contact line. The pressure gradient along the helical tube can be obtained from the pressure at two different holes on the contact line. The friction factor λ is defined by the following equation:

$$\lambda = \frac{\Delta p}{L}\frac{2d}{\rho w^2}$$

where Δp is the pressure drop between two pressure holes on the contact line, L the distance between these two holes (1400 mm or 700 mm), $d = 2a$ the tube diameter, and ρ the water density. The average axial velocity w is defined by the flux Q as

$$w = \frac{4Q}{\pi d^2}$$

The Reynolds number is defined by

$$\mathrm{Re} = \frac{dw}{\nu}$$

where ν is the kinematic viscosity.

Experimental results and discussion

Friction factor of the straight vinyl tube

In the present experiment three types of vinyl tube of different diameters to form helical tubes was used. The friction factor λ_s of each type of tube is first measured when tube is set in a straight line. If the inside surface of the tube is smooth enough, it will retain the same flow characteristics as a straight pipe. Fig. 5 shows the results. The open symbols in this figure mean the experimental data when the tube is smoothly connected with the outlet of the settling chamber, while the filled symbols stand for the data when there is a thin-plate circular orifice at the junction between the tube and the outlet of the settling chamber in order to disturb the flow. The height of the orifice is 6% of the tube diameter. The straight line denoted by 1 is drawn from the well-known Hagen-Poiseuille equation

$$\lambda_s = \lambda_H = \frac{64}{\mathrm{Re}} \tag{34}$$

which is valid for the laminar flow, and the straight line denoted by 2 shows the Blasius equation for the turbulent flow:

$$\lambda_s = \lambda_B = \frac{0.3164}{\mathrm{Re}^{0.25}} \tag{35}$$

The experimental results for all types of tube agree quite well with Eq. (34) for laminar flow and Eq. (35) for turbulent flow. This shows that the vinyl tube reinforced with a steel wire has a smooth inner surface. It is also seen that the transition to turbulence occurs at $\mathrm{Re} \simeq 2300$ when there is a thin-plate orifice at the inlet of the tube.

Friction factor of the helical tube

Fig. 6 shows the friction factor of the helical tube as a function of the Reynolds number for different torsion parameters β_0. Here, the straight curves 1 and 2 are drawn from Eqs. (34) and (35), respectively. The curve 3, which expresses the friction factor for laminar flow through a toroidal pipe ($\beta_0 = 0$), is drawn from equation obtained theoretically by Yanase, Goto, and Yamamoto (1989) [26] and this is given by

$$\lambda = \lambda_L = \lambda_H \left\{ 0.0938 \left[\mathrm{Re}\sqrt{\delta} \right]^{1/2} + 0.557 \right\}. \tag{36}$$

This equation is in good agreement with Hasson's experimental formula (see Berger et al. 1983 [2]) given by

$$\therefore \quad \lambda = \lambda_H \left\{ 0.0969 \left[\mathrm{Re}\sqrt{\delta} \right]^{1/2} + 0.556 \right\}. \tag{37}$$

The straight line denoted by 4 expresses Ito's equation (1959) [27] for turbulent flow through a toroidal tube ($\beta_0 = 0$) given by

$$\lambda = \lambda_T = \frac{0.316\sqrt{\delta}}{\left(\mathrm{Re}\,\delta^2\right)^{0.2}}. \tag{38}$$

In Eqs. (36) and (38), the local curvature δ is used instead of a/c in their original equations.

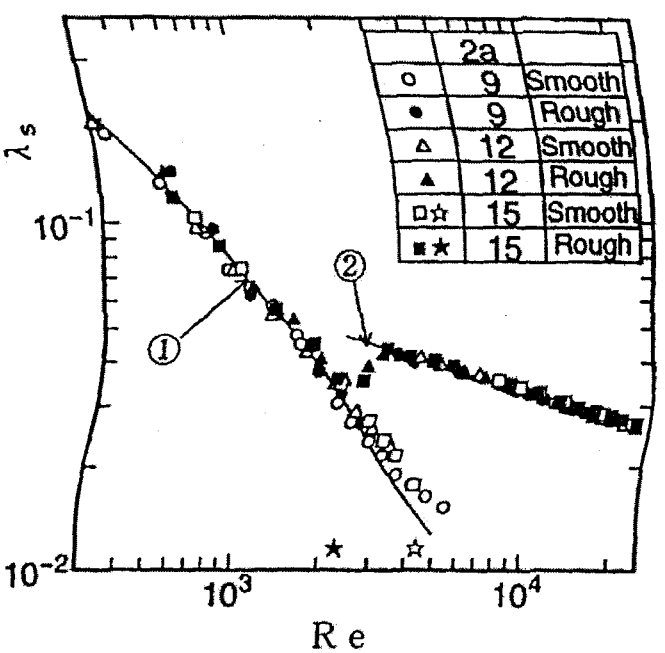

Fig. 5. Friction factor of straight tubes.

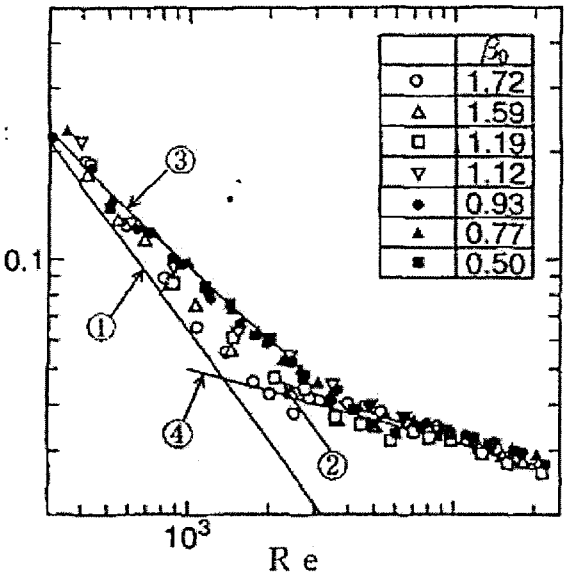

(a) $\delta_0 = 0.01$

Fig. 6. (a) Friction factor of helical tubes

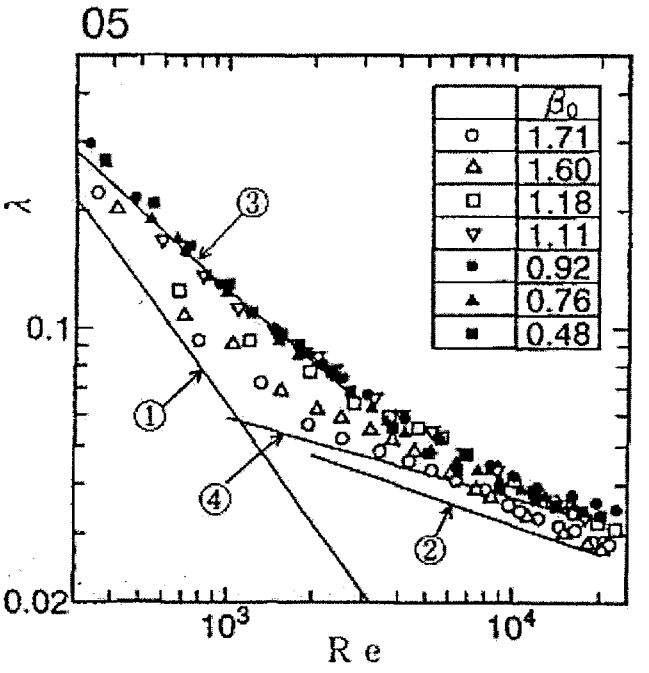

(b) $\delta_0 = 0.05$

Fig. 6. (b) Friction factor of helical tubes

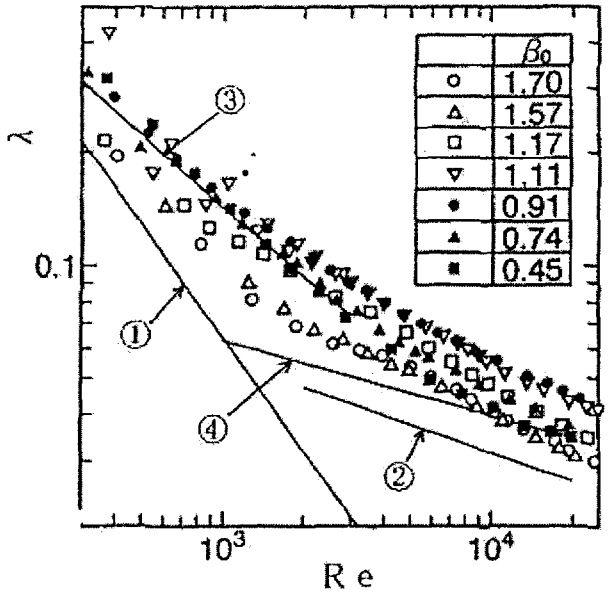

(c) $\delta_0 = 0.1$

Fig. 6. (c) Friction factor of helical tubes

When the flow is in a laminar state, the friction factor seems to be well described by Eq. (36) (or curve 3 for $\delta_0 = 0.01$ and 0.05, and $\beta_0 \leq 0.9$. The experimental data, however, lie a little bit above the curve 3 for $\delta_0 = 0.1$ and $\beta_0 \leq 1.1$. The friction factor then decreases and approaches that of a straight tube (Eq. (34)) for all δ_0 as β_0 increases further.

The friction factor of fully turbulent flow for which the Reynolds number may be greater than 8000 is in good agreement with Eq. (38) for the toroidal tube when β_0 is less than about 0.5. Thus, the friction factor increases more than Eq. (38) as β_0 increases in the range of $0.5 \leq \beta_0 \leq 1.1$. It decreases for further large β_0 toward the value of the straight tube. This tendency is clear for large δ_0.

6. Conclusion

- A set of Navier-Stokes equations in an arbitrary curvilinear coordinate system is obtained. According to the different values of the parameters k, τ helical circular pipes have four special types: straight pipe, planar curved pipe, twisted pipe and helical pipe.

- The form of Navier-Stokes equation for incompressible fluid flow in arbitrary curvilinear coordinate system may be advantageous to promote the theoretical and numerical research of flow through curved pipes. The effect of curvature and torsion on fully developed flow in pipe can be studied with help of these equations.

3. The semi-analytical solutions are found in the literature for the fully developed laminar flow in helical circular pipes.

- The results of experimental study of a helical tube flow are represented from [25]. This experiment covers laminar, transition, and turbulent flows for different cases of curvature and torsion of pipe. The data for the friction factor are demonstrated as well.

References

[1] Bara B, Nandakumar K, Masliyah JH. An experiment and numerical study of the Dean problem: flow development towards two-dimensional multiple solutions. J Fluid Mech 1992; 244: 339 - 76.

[2] Berger SA, Talbot L., Yao L.S. Flow in curved pipe. Ann. Rev Fluid Mech 1983; 15:461 - 512.

[3] Trefethen LM, Panton RL.. Some unanswered questions in fluid mechanics. Appl Mech Rev 1990; 43(8):153 - 70.

[4] Dean WR, Note on the motion of fluid' curved pipe. Phil Mag 1927;4(7) :208 - 23.

[5] Murata S, Miyake Y, Inaba T, Ogawa H. Laminar flow in helical pipe. Bull JSME 1981;24:355 - 62.

[6] Wang CY. On the low-Reynolds-number flow in helical pipe. J. Fluid Mech. 1981;108:185 - 94.

[7] Germano M. On the effect of torsion on helical pipe flow. J Fluid Mech. 1982; 125:1 - 8.

[8] Masliyah JH, Nandakumar K. Steady laminar flow through twisted pipes - fluid flow in square tubes. ASME J Heat transfer 1981; 103:785 - 90.

[9] Kao HC. Torsion effects on fully developed flow in a helical pipe. J Fluid Mech, 1987; 184:335 - 56.

[10] Tuttle ER. Laminar flow in twisted pipes. J Fluid Mech. 1990;219:545 - 70.

[11] Chen WH, Jan R. The characteristics of laminar flow in helical circular pipe. J Fluid Mech 1992; 244:241 - 56.

[12] Finlayson BA. The method of weighted residuals and variational principles. New York: Academic Press; 1972.

[13] Fan DN, Xu ZG. Tensorial Fluid Mechanics. Space Graphics Inc., 1983.

[14] Demuren AO, Rodi W. Calculation of turbulence-driven secondary motion in non-circular ducts. 5 Fluid Mech. 1984; 140:189 - 222.

[15] Ward-Smith AJ. Internal fluid flow. Oxford: Clarendon Press; 1980.

[16] Winters KH. A bifurcation study of laminar flow in a curved tube of rectangular cross-section. J Fluid Mech 1987;180:343 - 69.

[17] Selmi M, Nandakumar K, Finlay WH. A bifurcation study of viscous flow through rotating curved duct. J Fluid Mech 1994; 262:353 - 75.

[18] Germano M. The Dean equations extended to a helical pipe flow, J. Fluid Mech. , **203**, 1989; pp.289-305.

[19] Dean W.R., Note on the motion of a fluid in a curved pipe, *Phil. Mag.* 4, 208-233 (1927).

[20] Dean W.R., The streamline motion of a fluid in a curved pipe, *Phil. Mag.* 5, 673-693 (1928).

[21] Chen, W.H., Fan, C.N., 1986. Finite element analysis of incompressible viscous ¯ow in a helical pipe. Comput. Mech. 1, 281-292.

[22] Xie, D.E., 1990. Torsion effect on secondary flow in a helical pipe. Int. J. Heat and Fluid Flow, 11, 114-119.

[23] Liu, S., Masliyah, J.H., 1993. Axially invariant laminar flow in helical pipes with a finite pitch. J. Fluid Mech. 251, 315-353.

[24] Yamamoto, K., Yanase, S., Yoshida, T., 1994. Torsion effect on the flow in a helical pipe. Fluid Dyn. Res. 14, 259-273.

[25] Yamamoto, K., Akita, T., Ikeuchi, H., Kita, Y., 1995. Experimental study of the flow in a helical circular tube. Fluid Dyn. Res. 16, 237-249.

[26] Yanase S., N. Goto and K. Yamamoto (1989) Dual solutions of the flow through a curved tube, *Fluid Dynamics Res. 5,*191-201

[27] Ito H. (1959) Friction factors for turbulent flow in curved pipes, J. *Basic Engineering 81,* 123-134.

APPENDIX -A. (BIODATA)

Name: Dr. Nikolay P. Moshkin

Current Position: Associate Professor of Mathematics

Educational Background:

1974 Master's (MS Science Mathematics) Novosibirsk State U. Russia.

1983 Doctoral Ph.D. Fluid Mechan. Institut of Theoretical and Applied Mechanics of RAS, Novosibirsk, Russia

Fields of Specialization and Publications:

Numerical methods, Computational fluid dynamics

Over 60 research papers. Some of latest are

1. G.G.Chernykh, A.G.Demenkov, N.P.Moshkin, O.F.Voropaeva, Numerical Models of Turbulent Wakes in Homogeneous and Stratified Fluids. Computational Fluid Dynamics'96, Proceedings of the Third ECCOMAS computational Fluid Dynamics Conference, 9-13 September 1996, Paris, France, John Wiley & Sons, Ltd., pp.160-166.
2. Chernykh G.G., Moshkin N.P., Rychkova E.V., Tuchkov S.A., Comparison of some numerical algorithms for two-dimensional convection of fluid with nonlinear viscosity. International conference on the methods of aerophysical research, September 2-6, 1996, Novosibirsk, Russia, Proceedings, part 1, Novosibirsk 1996, pp. 79-84.
3. N.P. Moshkin, G.G. Chernykh, O.F.Voropaeva .Numerical models of turbulent Wakes in Stratified Fluids. Presented at the Fourth International Conference on Computational Physics, 2-4 June 1997, Singapore.
4. N.P.Moshkin, Numerical model to study natural convection in a rectangular enclosure filled with two immiscible fluids. International Journal of Heat and Fluid Flow, 2002, 23, pp.373-379.
5. N.P.Moshkin, P. Mounnamprang, Numerical Simulation of vortical ideal fluid flow through curved channel. International Journal for Numerical Methods in Fluidsm 2003, **41**, pp. 1173-1189.
6. O.F. Voropayeva, N.P. Moshkin, G.G. Chernykh, Internal waves generated by turbulent wakes in a stable-stratified medium, Dolady Physics, Translated from Doklady Academii Nauk, (to appear).

Research Experience in Thailand:

Completed Research Projects:

"Application of Group Analysis to Kinetic Equations / coinvestigator Project begun in March 1997—Funded for 2 years.

"Mathematical Modeling of steady natural convection in a two-layer system", Project begun in October 1998- Funded for 1 year.